Magazine of Civil Engineering

ISSN 2071-0305

journal homepage: http://engstroy.spbstu.ru/

DOI: 10.18720/MCE.94.1

The strength of short compressed concrete elements in a fiberglass shell

A.L. Krishan[a], M.Yu Narkevich[a*], A.I Sagadatov[a], V.I Rimshin[b]

[a] Nosov Magnitogorsk State Technical University, Magnitogorsk, Russia

[b] National Research Moscow State Civil Engineering University, Moscow, Russia

** E–mail: Narkevich_MU@mail.ru*

Keywords: columns (structural), concretes, elasticity, fiber reinforced plastics, fibers, filament winding, stress-strain curves, structural design, tubes (components)

Abstract. Experimental studies of short axially compressed cylindric elements with various indirect concrete reinforcements – fiberglass shells, steel spirals, and the joint use of these two types of reinforcement – have been carried out. The results of the experiments performed confirm the positive effect of both the outer fiberglass shell and spiral reinforcement on the strength of such elements. The highest strength was achieved with the simultaneous use of both types of indirect reinforcement. The presence of two types of indirect reinforcement significantly increased the deformability of the compressed elements under study. The maximum recorded values of the longitudinal deformations of shortening of such samples amounted to about 1.7 %. Such a high deformability of the compressed elements will allow to use high – strength longitudinal reinforcement efficiently in them. We list the main premises and dependencies of the method of deformational calculation of the strength of compressed concrete structures with indirect reinforcements. A performed comparison of the calculation results with experimental data indicates that the proposed method is perfectly suitable for practical use.

1. Introduction

The relatively rapid degradation of the strength properties of traditional building materials operating in aggressive environments is one of the main problems in the operation of buildings and structures in industry and civilian infrastructure.

Traditional building materials (steel, concrete, wood, brick and stone) have significant drawbacks that noticeably increase the cost of their maintenance, and reduce their service life. For example, it was estimated that in the United States repair and replacement of supporting building structures (piles, bridge supports, etc.) costs more than $ 1 billion annually [1].

We should also note that for load-bearing structures with external indirect reinforcement, such as concrete filled glass fiber-reinforced polymer tubes (CFGFT), the destruction of the external metal shell from corrosion can cause not only the destruction of the element, but also of the structure as a whole.

These circumstances force the search and use in building structures of modern, more advanced building materials with high physical and mechanical properties, low specific gravity, not subject to corrosion, rotting, warping; possessing chemical resistance, low combustibility, low coefficient of thermal linear expansion, a wide range of operating temperatures.

Some materials possess the required properties, namely, polymer composite materials (PCM) – polymer materials reinforced with fabrics, mats, strands or other forms of fibrous fillers (FRP). These materials are considered an attractive alternative for structures operating in marine and other aggressive environments, since they are resistant to the destruction mechanisms mentioned above.

Due to the advantages of FRP, researchers in many countries, including China, the USA, Canada, Japan, etc., are studying CFGFT with PCM shells. The strength and deformability of compressed CFGFT elements [2, 7, 8, 13–15, 17], as well as the use of compressed CFGFT elements in piles [3, 9–11], offshore platforms [4], sheet piling [5, 6], road constructions [12, 16]. In Russia, in connection with the adopted program for the introduction of composite materials, structures and products from them in the construction industry of

Krishan, A.L., Narkevich, M.Yu., Sagadatov, A.I., Rimshin, V.I. The strength of short compressed concrete elements in a fiberglass shell. Magazine of Civil Engineering. 2020. 94(2). Pp. 3–10. DOI: 10.18720/MCE.94.1

the Russian Federation (approved by the order of the Ministry of Regional Development of the Russian Federation No. 306 dated July 24, 2013), PCM production (pipes made of glass and carbon fiber, reinforcement for reinforcing reinforced concrete structures, woven materials, etc.) has grown significantly. However, today, there is a significant lag behind the USA, a number of European countries and China in the development of a regulatory framework for the design and calculation of building composite structures using PCMs, as well as noticeably less experience in the use of PCMs in building structures and the operation of such structures. The lack of domestic materials, technologies and equipment for the production of PCMs dictates a high price for the final product, thereby restraining their use.

However, increasing interest in the use of PCMs in construction, and a number of the above – mentioned measures of state support for manufacturers of composite materials, emphasize the relevance of the development and research of composite load – bearing building structures, such as, for example, CFGFTs.

In order to reduce the cost of compressed CFGFT elements, we propose to reduce the size of the outer fiberglass shell (wall thickness or pipe diameter), while maintaining the necessary bearing capacity through the use of high – strength concrete and (or) additional reinforcement of the concrete core. An analysis of the possible options for reinforcing the concrete core indicates that the use of spiral reinforcement will be most effective here [20, 21].

The purpose of this work is to evaluate the effectiveness of the spiral reinforcement of a high-strength concrete core of short compressed CFGFT elements.

2. Methods

In the course of laboratory studies, the strength of short CFGFT cylindrical samples under axial compression was evaluated. The cross – sectional diameter of the test samples was 109 mm; their length was 500 mm. In total, two series of sample elements were investigated. Each series consisted of 3 identical samples.

For the production of samples of series I, heavy concrete of class B80 was used. A fiberglass pipe was used as the outer shell for concrete. It had the following characteristics:

– section diameter of 109 mm;

– wall thickness of 4.5 mm;

– modulus of elasticity under axial tension (compression) E_{pl} = 13.8 GPa;

– modulus of elasticity at circumferential tension E_{pt} = 22.8 GPa;

– axial tensile strength f_{pl} = 265 MPa;

– tensile strength at circumferential tension f_{po} = 303 MPa;

– Poisson's ratio υ_{po} = 0.39;

– volumetric weight γ_p = 19.5 kN/m^3.

Series II differed from Series I only by the presence of spiral reinforcement of the concrete core. Before molding samples of this series, a reinforcing cage was placed inside the fiberglass pipe. A wire with a diameter of 5 Vr500 served as spiral reinforcement of the frame, which was wound with a pitch of 30 mm around four longitudinal rods made of wire of the same class – diameter 5 Vr500. The diameter of the cross section of the spiral was 90 mm. The yield strength of reinforcing wire is σ_{ys} = 552 MPa.

Series III consisted of reinforced concrete elements with a cross – sectional diameter of 100 mm. Prototypes of this series had indirect reinforcement similar to the series II, but they did not have fiberglass shells.

To obtain more objective data, when comparing the strength of samples of the structures under study, three samples of different series were simultaneously formed using concrete mix of one batch.

After manufacturing, all the prototypes were kept at a temperature of about 20 °C for 28 days. The tests were carried out on a 500 – ton hydraulic press with a short – term compressive load. The load was transmitted over the entire cross section of the structures. In this case, a standard technique was used, regulated by Russian State Standard GOST 8829.

3. Results and Discussion

The main results of the experiments are summarized in Table 1. It contains the following data for each sample:

– prismatic strength of the source concrete f_c;

– percentage of fiberglass reinforcement μ_p;

– percentage of spiral reinforcement μ_{sc};

– breaking load $N_u^{\exp}$;

– the force that the sample could withstand under conditions of uniaxial compression N_{cp};

– indirect reinforcement efficiency coefficient $m_{eff} = N_u^{\exp} / N_{cp}$;

– relative limit of elastic work $n_{el} = N_{el}^{\exp} / N_u^{\exp}$, where $N_{el}^{\exp}$ is maximum effort corresponding to the stage of elastic work;

– limitary axial deformation of shortening $\varepsilon_u^{\exp}$.

Table 1. Main laboratory test results.

Sample	f_c, MPa	μ_p, %	μ_{sc}, %	$N_u^{\exp}$, kN	N_{cp}, kN	m_{eff}	n_{el}	$\varepsilon_u^{\exp}$, %
I-1	82.9	18.8	0	967	651	1.48	0.49	0.65
I-2	84.6	18.8	0	1033	664	1.55	0.54	0.75
I-3	85.0	18.8	0	1000	667	1.50	0.52	0.80
II-1	82.9	18.8	1.45	1300	694	1.87	0.52	1.70
II-2	84.6	18.8	1.45	1300	708	1.84	0.58	1.57
II-3	85.0	18.8	1.45	1380	711	1.94	0.60	1.80
III-1	82.9	0	1.45	867	651	1.33	0.55	0.55
III-2	84.6	0	1.45	833	664	1.25	0.51	0.50
III-3	85.0	0	1.45	900	667	1.35	0.56	0.48

An analysis of the results indicates that indirect reinforcement (fiberglass shell and / or spiral reinforcement) had a significant effect on the strength of centrally compressed samples. Explicitly, the presence of just spiral reinforcement led to an increase in their strength compared to uniaxially compressed elements by an average of 1.31 times, the presence of a fiberglass shell – by 1.51 times, and the presence of both types of indirect reinforcement – by 1.88 times.

The relative limit of elastic work for the samples of series II turned out to be higher than for samples of other series, but not by much. Compared to the samples of series I, it is 5–10 % higher, and compared to the samples of series III, the difference in n_{el} values is even less.

The maximum recorded values of the longitudinal deformations $\varepsilon_u^{\exp}$ of the samples under study significantly depended on the level of indirect reinforcement. The smallest value of these deformations was recorded in samples of series III. Their $\varepsilon_u^{\exp}$, on average, amounted to 0.63 %, which is approximately two and a half times higher than similar deformations of uniaxially compressed concrete. The limit deformations of series I samples turned out to be 22 % higher. The highest deformability was demonstrated by samples in a fiberglass shell with spiral reinforcement of concrete. For them, the average value was 1.69 %. It should be noted here that the high deformability of the compressed elements makes it possible to use high – strength longitudinal reinforcement efficiently in them.

The nature of the destruction of the studied samples mainly depended on the presence of an outer shell. For reinforced concrete elements with spiral reinforcement, before reaching the maximum load, almost complete destruction of the protective layer was observed (Figure 1, c). With a further increase in load, the concrete core crushed inside the spiral.

The destruction process of samples of series I and II was different. Immediately before the destruction, a slight bulging of the outer shell was observed. The reason for this was the fragmentation of the concrete core in local zones, due to the beginning of the shift of its parts. With a further increase in load, a rupture of the fiberglass shell was observed (Figure 1, a, 1, b). The nature of the destruction of the samples of both series was fragile. Externally, the picture of the destroyed samples practically did not differ. However, the presence of spiral reinforcement in Series II samples slightly decreased fragility due to a significant increase in the limit of deformability.

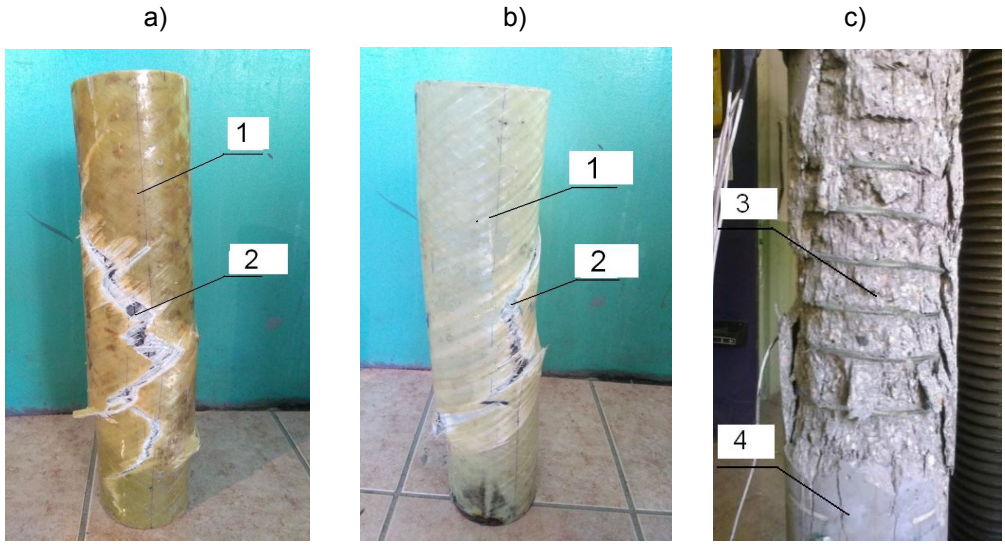

Figure 1. The nature of the destruction of samples from the series I (a), II (b) and III (c): 1 – not destroyed area; 2 – shell rupture at an angle of 30–60 degrees to the longitudinal axis; 3 – peeling of the protective layer of concrete; 4 – vertical cracks in the protective layer of concrete.

Strength calculation of test samples

In this paper, we study the force resistance of short samples of little flexibility. Their destruction occurs from a loss of compressive strength.

In modern publications, there are proposals for the calculation of such structures based on the breaking stress method [18]. In this case, the volumetric stress state of the materials is taken into account using empirical dependencies having a limited area of applicability. There are publications listing the results of calculations of compressed concrete elements based on finite element models [18–20]. Sadly, neither of the published works takes into account the actual nature of the force resistance of compressed elements with indirect reinforcement. In particular, they ignore the fact of a change in lateral pressure on the concrete core during a gradual increase in load, which causes a constant change in the stress state of the materials.

Considering this, we propose to calculate the strength of CFGFT using a different approach. The nature of their reinforcement involves the use of a deformation model for this purpose [21].

The essence of the proposed deformational calculation of the strength of centrally compressed elements is as follows. An element is considered, at the ends of which compressive load N with a random eccentricity e_a is applied. Before that, the concrete core and the outer shell (if applicable) of the element is divided into small ranges with areas A_{cj} and A_{pk}, within which the emerging stresses are averaged. The area of each rod of longitudinal reinforcement (if applicable) is indicated as A_{sn}.

In the calculation, the axial deformations of the most compressed fiber are increased step by step, starting from zero. In accordance with the Bernoulli hypothesis, a strain diagram is constructed in the cross section of an eccentric compressed element corresponding to the equilibrium conditions of internal forces in concrete, fiberglass, and forces from external load. To check the equilibrium conditions by the values of deformations in each section of concrete and fiberglass outer shell, into which the normal section of the element was previously divided, we calculate the stresses σ_{czj}, σ_{pzk} and σ_{szn}. The equilibrium conditions in the general case are written in the form of a system of equations:

$$N \cdot e_a = \sum_j \sigma_{czj} A_{cj} Z_{cj} + \sum_k \sigma_{pzk} A_{pk} Z_{pk} + \sum_n \sigma_{szn} A_{sn} Z_{sn}; \quad (1)$$

$$N = \sum_j \sigma_{czj} A_{cj} + \sum_k \sigma_{pzk} A_{pk} + \sum \sigma_{szn} A_{sn}, \quad (2)$$

where Z_{cj}, Z_{pk} and Z_{sn} are coordinates of the center of gravity of the j-th section of concrete, the k-th section of the fiberglass outer shell (if applicable) and the n-th rod of longitudinal reinforcement (if applicable).

When the equality of the left and right sides in Equations (1) and (2) is observed, the compressive force from the external load is fixed and the deformation build – up process continues $\varepsilon_{cz,\max}$. The calculation continues until the compressive force reaches its maximum value N_u or until axial deformation reaches the maximum permissible value $\varepsilon_{cz,u}$, set by the researcher (see Figure 2).

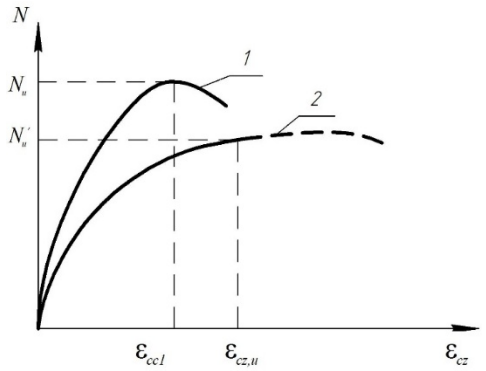

Figure 2. Dependencies «$N - \varepsilon_{cz}$»: 1 is when N reaches its maximum value; 2 is when ε reaches its set value.

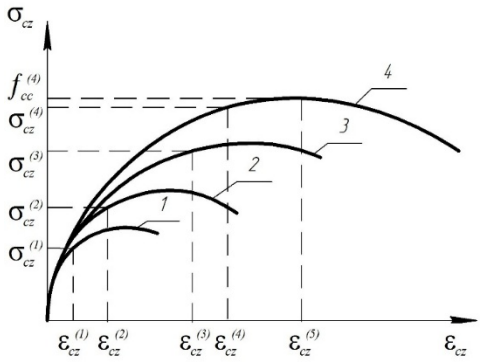

Figure 3. Concrete deformation diagrams for incremental longitudinal deformation: *1* – uniaxial compression, 2, *3* – volumetric compression at intermediate stages of deformation, *4* – volumetric compression in the limiting state.

The deformation calculation involves the use of deformation diagrams of the materials from which the structure under consideration is made. In our case, it is necessary to have diagrams reflecting the dependences between stresses and strains of axial direction for volumetrically stressed concrete and shell «$\sigma_{cz} - \varepsilon_{cz}$» and «$\sigma_{pz} - \varepsilon_{pz}$». Longitudinal reinforcement deformation diagram «$\sigma_{sz} - \varepsilon_{sz}$» can be adopted according to the recommendations of current standards. The accuracy of the calculations largely depends on the reliability of the adopted diagrams. In this case, the most difficult task is to build a diagram of concrete deformation.

Numerous proposals in publications on this subject [21, 22, 27–31] do not provide a reliable estimate of the strength resistance of a concrete core. They offer analytical dependences for describing the deformation diagrams of volumetric compressed concrete when a lateral pressure of a certain value is applied to it. Pressure is most often taken for the limit state of the structure. In fact, the lateral pressure is constantly changing with increasing load level. To each side pressure $\sigma_{cr}^{(i)}$ at a particular i-th step of the calculation, there is a corresponding strain diagram. Taking into account the constant change in lateral pressure, we can obtain multiple diagrams «$\sigma_{cz}^{(i)} - \varepsilon_{cz}^{(i)}$» (see Figure 3). This fact significantly complicates the deformation strength calculation, but it cannot be ignored.

To construct such strain diagrams, we propose to view the concrete core as a transversely isotropic body. The outline of each diagram is assumed to be curved with upward and downward sections. In this setting, for the analytical description of the diagrams, the most important task is to determine the coordinates of the vertices – the maximum stress $f_{cc}^{(i)}$ and corresponding deformation $\varepsilon_{cc1}^{(i)}$.

According to previously performed theoretical studies [32, 23], the maximum stress $f_{cc}^{(i)}$ and deformation $\varepsilon_{cc1}^{(i)}$ of volumetric compressed concrete corresponding to lateral pressure is calculated using the following formulas:

$$f_{cc}^{(i)} = f_c \left(\frac{3\bar{\sigma}_i + 2}{4} + \sqrt{\left(\frac{\bar{\sigma}_i - 2}{4} \right)^2 + \frac{\bar{\sigma}_i}{b}} \right); \tag{3}$$

$$\varepsilon_{cc1}^{(i)} = \alpha_{ci} \left[\varepsilon_{c1} \alpha_{ci}^{1.5} - \frac{f_c}{E_c} \left(\alpha_{ci}^{1.5} - 1 \right) \right], \tag{4}$$

where $\bar{\sigma}_i$ is a relative value of lateral pressure from the outer shell to the concrete core $\bar{\sigma}_i = \sigma_{cr}^{(i)} / f_c$;

b is material coefficient, which is an experimental value (for heavy concrete b = 0.096 [24]);

ε_{c1} is relative strain of uniaxially compressed concrete under stress f_c;

α_{ci} is coefficient of strength growth of volumetrically compressed concrete $(\alpha_{ci} = f_{cc}^{(i)} / f_c)$.

The relationship between stress and strain $\sigma_{cz}^{(i)} - \varepsilon_{cz}^{(i)}$ can be adopted according to the proposal of M. Attard and S. Setung [25], or a slightly modernized formula of D. Mander [16], which is written in the following form

$$\sigma_{cz}^{(i)} = f_{cc}^{(i)} \frac{\lambda^{(i)} \frac{\varepsilon_{cz}^{(i)}}{\varepsilon_{cc1}^{(i)}}}{\lambda^{(i)} - 1 + \left(\frac{\varepsilon_{cz}^{(i)}}{\varepsilon_{cc1}^{(i)}} \right)^{\lambda^{(i)}}}, \quad (5)$$

where $\lambda^{(i)}$ is a coefficient calculated by the following formula:

$$\lambda^{(i)} = \frac{E_c}{E_c - f_{cc}^{(i)} / \varepsilon_{cc1}^{(i)}}, \quad (6)$$

where E_c is initial modulus of elasticity of concrete.

To find the lateral pressure on concrete from the fiberglass shell, the following formula was proposed in [16]

$$\sigma_{cr}^{(i)} = \frac{\upsilon_{zr}^{(i)} - \upsilon_p^{(i)}}{\frac{d}{2E_{pc}t} + \frac{1 - \upsilon_{zr}^{(i)}}{\nu_{cz}^{(i)} E_c}} \cdot \varepsilon_{cz}^{(i)}. \quad (7)$$

where $\upsilon_{zr}^{(i)}$ and $\upsilon_p^{(i)}$ are lateral deformation coefficients of concrete and fiberglass;

$\nu_{cz}^{(i)}$ is the coefficient of elasticity of concrete;

E_{pc} is modulus of elasticity of the steel shell in compression;

d and t are external diameter and wall thickness of the steel shell

The coefficient of elasticity of concrete introduced into this formula to refine the calculation in the zone of large deformations is determined by the formula

$$\nu_{cz}^{(i)} = \frac{\sigma_{cz}^{(i)}}{E_c \varepsilon_{cz}^{(i)}}. \quad (8)$$

To simplify the calculations, the fiberglass shell can be considered as an elastic isotropic material. In this setting $\upsilon_p^{(i)} = \upsilon_{po}$, where υ_{po} is Poisson's ratio of fiberglass.

The transverse strain coefficient of concrete varies. As the stress level increases, it increases from the Poisson's ratio υ_{co} = 0.18÷0.25 to the limit value $\upsilon_{zru}^{(i)}$ at the stage of concrete destruction.

In [23], to determine the current values of $\upsilon_{jr}^{(i)}$ ($j = z, r$) by A.L. Krishan offered the following formula:

$$\upsilon_{zr}^{(i)} = \upsilon_{zru}^{(i)} - (\upsilon_{zru}^{(i)} - \upsilon_{co}) \left(\frac{\nu_{cz}^{(i)} - \nu_{czu}^{(i)}}{1 - \nu_{czu}^{(i)}} \right)^{0.5}. \quad (9)$$

The limit value of the coefficient of transverse deformation for a concrete core is determined by the formula

$$\upsilon_{zru}^{(i)} = \upsilon_{co} + (1 - \sqrt[3]{\nu_{czu}^{(i)}}), \quad (10)$$

where $\nu_{czu}^{(i)}$ is the coefficient of elasticity of the concrete core at the top of the diagram of its deformation, calculated by the formula (8) with $\sigma_{cz}^{(i)} = f_{cc}^{(i)}$ and $\varepsilon_{cz}^{(i)} = \varepsilon_{cc1}^{(i)}$.

Based on the proposed method of deformation calculation, an algorithm and a computer program «CFST-18» have been developed, which allow us to evaluate the stress-strain state and determine the

strength of compressed concrete elements. Table 2 shows a comparison of the new experimental values of strength and ultimate axial deformations of the samples studied by the authors of the article with the results of calculations using this program. Here, for analysis, calculated data are given on the total percentage of indirect reinforcement μ, the strength of volumetrically compressed concrete f_{cc}^{th}, as well as lateral pressure σ_{cr}^{th} in the limiting state of the element.

Table 2. Comparison of experimental data with calculation results.

Series	μ, %	f_c, MPa	σ_{cr}^{th}, MPa	f_{cc}^{th}, MPa	$\alpha_c = \frac{f_{cc}^{th}}{f_c}$	N_u^{th}, kN	$\frac{N_u^{\exp}}{N_u^{th}}$	ε_u^{th}, %	$\frac{\varepsilon_u^{\exp}}{\varepsilon_u^{th}}$
I-1	18.8	82.9	2.2	115.8	1.40	933	1.04	0.63	1.03
I-2	18.8	84.6	2.3	117.9	1.39	957	1.08	0.62	1.21
I-3	18.8	85.0	2.3	118.5	1.39	962	1.04	0.62	1.29
II-1	20.25	82.9	4.4	136.2	1.64	1440	0.90	1.92	0.88
II-2	20.25	84.6	4.4	138.9	1.64	1482	0.88	1.89	0.83
II-3	20.25	85.0	4.4	139.4	1.64	1490	0.93	1.88	0.96
III-1	1.45	82.9	4.0	126.7	1.53	826	1.05	0.44	1.25
III-2	1.45	84.6	4.0	129.1	1.53	845	0.98	0.42	1.19
III-3	1.45	85.0	4.0	129.6	1.52	850	1.06	0.42	1.14

Based on the comparison, we can state that the proposed calculation method allows to obtain quite reliable results on the strength and deformability of compressed elements with different options for indirect reinforcement. The maximum difference between the experimental and theoretical values of strength was 12 %. Moreover, such a discrepancy is observed for samples in which lateral deformations of concrete are restrained by both the outer shell and spiral reinforcement. Theoretical and experimental values of limit strains differ more significantly. The difference between them is in the range of +19 to –21 %. However, specialists know that such differences should be considered quite acceptable for deformations. Therefore, in general, we can state that the performed comparison confirmed the adequacy of the adopted calculation model.

4. Conclusions

1. The results of experimental studies indicate a positive effect on the strength of short compressed CFGFRT elements of both options used indirect reinforcement – the outer fiberglass shell and spiral reinforcement.

2. The high strength of such samples is due to a significant increase in concrete strength, which in samples with two types of indirect reinforcement increased by about 64 %.

3. The simultaneous presence of two types of indirect reinforcement significantly increased the deformability of the studied compressed elements. The maximum recorded values of longitudinal deformations of shortening of series II specimens amounted to about 1.7 %.

4. The high deformability of the compressed elements allows the efficient use of high-strength longitudinal reinforcement in them, which has economic feasibility.

5. The proposed calculation method allows obtaining reliable results on the strength and deformability of compressed elements with different options for indirect reinforcement.

References

1. Lampo, R., Maher, A., Busel, J., Odello, R.. Design and development of FRP composite piling systems. Proceedings, International Composites Expo, 1997. Nashville. TN. Pp. 16–18.
2. Fam, A.Z., Rizkalla ,S.H. Concrete – filled FRP tubes for flexural and axial compression. Proceedings, 3rd International Conference on Advanced Composite Materials in Bridges and Structures. Ottawa. Canada, 2000. Pp. 315–322.
3. Fam, A.Z., Pando, M.A., Filz, G., Rizkalla, S.H. Precast Piles for Route 40 Bridge in Virginia Using Concrete Filled FRP Tubes. PCI Journal, Precast/Prestressed Concrete Institute. 48(3), May – June 2003. Pp. 32–45.
4. API. Recommended practice for planning, designing and constructing fixed offshore platforms – Working stress design. 20th Edition. American Petroleum Institute. Washington, DC, 1993.
5. Ashford, S.A., Jakrapiyanun, W. Drivability of Glass FRP Composite Piling. Journal of Composites for Construction. 2001. 5(1). Pp. 58–60.
6. Chin, J., Nguyen, T., Aouadi, K. Effects of environmental exposure on fiber – reinforced plastic (FRP) materials used in construction [Online]. Composites Technology & Research. URL: https://doi.org/10.1520/CTR10120J
7. El – Tawil, S., Deierlein, G. Strength and ductility of concrete encased composite columns. Journal of Structural Engineering. 1999. 125(9), Pp. 1009–1019.
8. Fardis, M., Khalili, H. Concrete encased in fiberglass plastic. ACI Proceedings, 78, Document JL78 – 38, 1981. Pp. 440–446.
9. Iskander, M., Hassan, M. State of the practice review in FRP composite piling. Journal of Composites for Construction. ASCE. 1998. 2(3). Pp. 116–120.

10. Pando, M., Lesko, J., Case, S.. Preliminary Development of a Durability Model for concrete – filled FRP piles. Proceedings, 46th International Society for the Advancement of Material and Process Engineering (SAMPE) Conference. Long Beach. CA, 2001. Pp. 1597–1611.
11. Pando, M., Lesko, J., Fam, A., Rizkalla, S. Durability of Concrete-filled Tubular FRP Piles. Proceedings, 3rd International Conference on Composites in Infrastructure (ICCI) [Online]. Conference. San Francisco. URL: https://ru.scribd.com/document /335007153/Durability-of-Concrete-Filled-Tubular-FRP-Piles-Paper-12-pdf
12. Ballinger, C. Composites poised to make inroads as highway structural materials. The Journal: Roads and Bridges, April 1994. Pp. 40–44.
13. Fam, A.Z., Rizkalla, S.H. Behavior, S.of axially loaded concrete – filled circular fiberreinforced polymer tubes. ACI Structural Journal. 2001. 98(3). Pp. 280–289.
14. Narkevich, M.Yu., Sagadatov, A.I. Study of the operation of centrally compressed steel – concrete elements with a core of high – strength concrete and thin – walledshell. BST: Bulletin of construction equipment. 2017. No. 11 (999). Pp. 14–15.
15. Krishan, A.L., Rimshin, V.I., Astafyeva, M.A., Narkevich, M.Yu. Determination of deformation characteristics of concrete. Natural and technical sciences. 2014. No. 9–10 (77). Pp. 367–369.
16. Krishan, A.L., Rimshin, V.I., Telichenko, V.I., Rakhmanov, V.A., Narkevich, M.Yu. The practical implementation of the calculation of concrete columns [Online]. Technology of the textile industry. 2017. 2(368). Pp. 227–232. URL: http://ttp.ivgpu.com/wp-content/uploads/2017/07/368_50.pdf
17. Fattah, A. Behaviour of concrete columns under various confinement effects. A dissertation doctor of philosophy. USA: Kanzas State University. Kanzas, 2012. 399 p.
18. Ahmed, M., Liang, Q., Patel, V., Hadi, M. Numerical analysis of axially loaded circular high strength concrete-filled double steel tubular short columns [Online]. Thin-Walled Structures. 2019. 138. Pp. 105–116. URL: https://doi.org/10.1016/j.tws.2019.02.001
19. Wang, G., Shen, Q., Jiang, H., Pan, X. Analysis and Design of Elliptical Concrete-Filled Thin-Walled Steel Stub Columns Under Axial Compression [Online]. International journal of steel structures. 2018. 18(2). Pp. 365–380. URL: https://link. springer.com/article/10.1007/s13296-018-0002-5
20. Wang, F., Han, L. Analytical behavior of special-shaped CFST stub columns under axial compression [Online]. Thin-Walled Structures. 2018. 129. Pp. 404–417. URL:https://doi.org/10.1016/j.tws.2018.04.013
21. Teng, J., Jiang, T., Lam, L., Luo, Y. Refinement of a design-oriented stress-strain model for FRP-Confined concrete [Online]. Journal Composites of Construction, ASCE. 2009. 13(4). Pp. 269–278. URL: https://doi.org/10.1061/(ASCE)CC.1943-5614.0000012
22. Wei, Y., Wu, Y. Unified stress-strain model of concrete for FRP-confined columns [Online]. Journal of Construction and Building Materials. 2012. 26(1). Pp. 381–392. URL: https://doi.org/10.1016/j.conbuildmat.2011.06.037
23. Krishan, A.L., Astafeva, M.A., Chernyshova, E.P. Strength Calculation of Short Concrete-Filled Steel Tube Columns [Online]. Journal of Concrete Structures and Materials. 2018. 84(12). URL: https://doi.org/10.1186/s40069-018-0322-z.
24. Karpenko, N.I., Karpenko, S.N., Petrov, A.N., Palyuvina, S.N. Model deformirovaniya zhelezobetona v prirashcheniyakh i raschet balok-stenok i izgibayemykh plit s treshchinami. Petrozavodsk: Izd-vo PetrGU, 2013. 156 p.
25. Attard, M., Setunge, S. Stress-strain relationship of confined and unconfined concrete [Online]. ACI Mater J. 1996. 93(5). Pp. 432–442. URL: https://www.concrete.org/publications/internationalconcreteabstractsportal.aspx?m=details&ID=9847
26. Krishan, A.L., Narkevich, M.Yu., Sagadatov, A.I. Experimental investigation of selection of warm mode for high-performance self-stressing self-compacting concrete [Online]. 7th International Symposium on Actual Problems of Computational Simulation in Civil Engineering (APCSCE). Russia, Novosibirsk, 2018. Pp. 1–6. URL: https://doi.org/10.1088/1757-899X/456/1/012049
27. Younesi, A., Rezaifar, O., Gholhaki, M., Esfandiari A. Structural health monitoring of a concrete-filled tube column. Magazine of Civil Engineering. 2019. No. 1(85). Pp. 136–145. DOI: 10.18720/MCE.85.11.
28. Snigireva, V.A., Gorynin, G.L. The nonlinear stress-strain state of the concrete-filled steel tube structures. Magazine of Civil Engineering. 2018. 83(7). Pp. 73–82. DOI: 10.18720/MCE.83.7.
29. Vatin, N.I., Barabanshchikov, Yu.G., Komarinskiy, M.V., Smirnov, S.I. Modification of the cast concrete mixture by air-entraining agents. Magazine of Civil Engineering. 2015. 56(4). Pp. 3–10. DOI: 10.5862/MCE.56.1. (rus)
30. Barabanshchikov, Yu.G., Arkharova, A.A., Ternovskii, M.V. Concrete with the lowered shrinkage and creep. Construction of Unique Buildings and Structures. 2014. 22(7). Pp. 152–165. DOI: 10.18720/CUBS.22.12. (rus)
31. Barabanshchikov, Yu.G., Komarinski, M.V. Superplasticized technological properties of concrete mixtures. Construction of Unique Buildings and Structures. 2014. 21(6). Pp. 58–69. DOI: 10.18720/CUBS.21.4. (rus)
32. Krishan, A.L., Troshkina, E.A., Chernyshova, E.P. Strength of Short Centrally Loaded Concrete-Filled Steel Tubular Columns [Online]. 18th IFAC Conference on Technology, Culture and International Stability TECIS 2018. Azerbaijan. Baku. 2018. Vol. 51. Iss. 30. Pp. 150–154. URL: https://www.sciencedirect.com/science/article/pii/S2405896318329380?via%3Dihub.

Contacts:

Anatolii Krishan, kris_al@mail.ru
Mikhail Narkevich, Narkevich_MU@mail.ru
Azat Sagadatov, azat0680@mail.ru
Vladimir Rimshin, v.rimshin@niisf.ru